ELSEVIER

Polymer 42 (2001) 3697–3702

polymer

www.elsevier.nl/locate/polymer

New observations on the optical properties of PPV/TiO$_2$ nanocomposites

Jing Zhang[a,*], Bo-jie Wang[b], Xin Ju[a], Tao Liu[a], Tian-dou Hu[a]

[a]*Beijing Synchrotron Radiation Facility, Institute of High Energy Physics, Chinese Academy of Sciences, Beijing 100039, People's Republic of China*

[b]*Institute of Chemistry, The Chinese Academy of Science, Beijing 100101, People's Republic of China*

Received 29 May 2000; received in revised form 18 September 2000; accepted 22 September 2000

Abstract

The optical properties of poly(phenylenevinylene) (PPV)/TiO$_2$ nanocomposites, prepared from mixtures of PPV precursor and titanium butoxide ethanol solution in a sol–gel process, are investigated by UV–VIS, FT-IR, PL spectroscopy and TEM. The TEM images showed that the TiO$_2$ nano-aggregates took the form of a sphere and finally ellipsoid with an alignment, as the content of TiO$_2$ increased. FT-IR spectra indicated that the titanium butoxide hydrolyzed to form Ti organic compound, which can result in the alignment structure of TiO$_2$ nanoparticles; at the same time, PPV in TiO$_2$ matrix had the *trans*-PPV configuration. PL spectra revealed that the light emission of the PPV/TiO$_2$ nanocomposites was from PPV, and the relative intensity of the vibrant components changed with the formation of the TiO$_2$ alignment structure. These phenomena suggest that the TiO$_2$ matrix can form confined environments to control PPV molecular aggregate states and further effect the optical property of PPV. © 2001 Elsevier Science Ltd. All rights reserved.

Keywords: Optical property; Poly(phenylenevinylene); TiO$_2$ nanoparticles

1. Introduction

Conjugated polymers are showing real promise in optic-electronic applications [1], in particular, poly(*p*-phenylenevinylene) (PPV) and its derivatives can be used as the photoactive layers in light emitting diodes (LED) [2–5], lasers [6–8] and photovoltaic cells [9]. These optical quality films can be cast from solution using common organic solvents, and benefit from the processability of polymers. The optical and electronic properties of PPV, however, still have to be improved. A feasible way to improve is to combine PPV with inorganic nanoparticles, for example, the incorporation of CdSe nanoparticles into PPV was used to make blue light emitters [10]. In addition, the PPV/CdSe nanocomposite showed the feature of enhanced luminescence [11]. More recently, it has been seen that TiO$_2$ nanoparticles blend with PPV could result in improving photovoltaic efficiency [12]. Therefore, it has been of considerable interest to study the effects of inorganic nanoparticles on the optical and electronic properties of PPV.

Generally it has been thought that these nanoparticles can act as charge carriers or electro-optically active centers to impact on the optical and electronic properties of PPV [13]. Yet, very little is known about the effect of the microenvironment of inorganic matrix upon the optical property of PPV. In our work, a series of PPV/TiO$_2$ nanocomposites are prepared in a sol–gel process. The relationship between the confined environments of TiO$_2$ matrix and optical property of PPV are investigated by ultraviolet–visible (UV–VIS), FT-IR and photoluminescence (PL) spectroscopy, and transmission electron microscopy (TEM).

2. Experimental

2.1. The preparation of PPV/TiO$_2$ nanocomposite

The precursor polymer to the PPV (Fig. 1) is prepared following the standard polyelectrolyte route [14], using α,α-dichloro-*p*-xylene and tetrahydrothiophene as the starting reactants. Polymerization is carried out in methanol, with tetrabutylammonium hydroxide as a base catalyst. At the end of the polymerization, the reaction was quenched by neutralizing the basic reaction mixture with dilute HCl(aq) (0.5 M), to a pH of ~4–6. The precursor polymer solution thus prepared was purified by dialysis (molecular weight cut-off (MWCO) of 3000) against methanol over a period of three days, with a daily change of fresh solvent. The obtained polymer is a colorless, viscous solution.

The sol solution of Titanium oxide was prepared by reacting Titanium butoxide (TBT) in ethanol with the required amount of HCl (1 N). An appropriate amount of the sol

---

* Corresponding author. Fax: +86-10-682-753-47.
E-mail address: jzhang@alpha02.ihep.ac.cn (J. Zhang).

PII: S0032-3861(00)00703-5

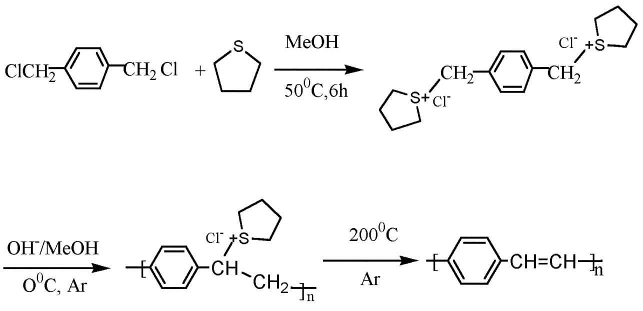

Fig. 1. Synthetic pathways to PPV.

solution was mixed with the PPV precursor, as listed in Table 1. After vigorous stirring, the solution was spin-coated onto the quartz glass and then heat-treated at 200°C in a stream of argon. Schematic diagram for the formation of the PPV/TiO_2 nanocomposite films from the PPV precursor polymer and TiO_2 sol solution was given in Fig. 2.

2.2. Measurements

The thickness of the PPV film and the PPV/TiO_2 nanocomposite films (80–100 nm) is determined with an Alpha-step200. UV–VIS absorption spectra of the PPV film and the PPV/TiO_2 nanocomposite films are measured using a Hitachi U-2001 spectra. A PERKIN ELMER LS50B spectrum is used to obtain PL spectra of the PPV film and the PPV/TiO_2 nanocomposite films. The morphologies of the composite films are observed by using JEM-100CX TEM.

3. Results

3.1. TEM

Fig. 3 showed TEM images of PPV/TiO_2 nanocomposites with different content of TiO_2. The brighter contrast can be ascribed to the PPV, while the darker regions indicated TiO_2 particles. When the TiO_2 content was 10%, the TiO_2 nanoparticles, whose size was 10 nm, aggregated to form the densely packed regions of the TiO_2 particles, which were surrounded by the regions of polymers being free from TiO_2 particles. As the TiO_2 content increased, the size of the TiO_2 particle domains became large, and the TiO_2 particles took the form of spheres. When the TiO_2 content was up to 50%, the TiO_2 particles aggregated in ellipsoid with alignment structure.

Table 1
The composition of PPV/TiO_2

Sample	PPV precursor weight ratio (%)	TiO_2 weight ratio (%)
PPV	100	0
PPV/TiO_2-A	91	9
PPV/TiO_2-B	70	30
PPV/TiO_2-C	60	40
PPV/TiO_2-D	50	50

3.2. FT-IR spectra

The chemical structures of PPV and all PPV/TiO_2 nanocomposite films were characterized with a FT-IR spectroscopy as shown in Fig. 4. The band near 963 cm^{-1} was due to C–H out-of-plane bending of the *trans* configuration of the vinylene group. The band near 3024 cm^{-1} was assigned to the *trans*-vinylene C–H stretching mode. The bands near 831 and 1515 cm^{-1} were assigned to *p*-phenylene C–H out-of-plane bending and C–C ring stretching, respectively. The above bands are the characteristic absorption of PPV, and shown in the spectra of both the PPV film and PPV/TiO_2 nanocomposite films. In PPV/TiO_2 nanocomposite films, the band at 3450 cm^{-1} was corresponded to the O–H stretching mode of Ti–OH; the bands near 1623 cm^{-1} and 1105 cm^{-1} was assigned to the Ti–O and Ti–O–C stretching mode. This indicated that TBT hydrolyzed to form Ti organic compound, which can result in the alignment structure of TiO_2 particles [15]. However, no absorption in the FT-IR spectra was observed in the vicinity of 630 cm^{-1} corresponding to the *cis*-CH bending mode, which showed that the composite systems did not change the nature of the elimination reaction, which yielded *trans*-PPV exclusively [16].

3.3. UV–VIS spectra

UV–VIS spectra of PPV and PPV/TiO_2 nanocomposites were depicted in Fig. 5. The rise of π–π^* absorption of PPV was at 510 nm, while the band-gap onset of TiO_2 was about 370 nm, and a peak occurred at 300 nm. The absorption of PPV in the composites was unperturbed by the presence of the TiO_2 nanoparticles, displaying the same π–π^* absorption as for PPV alone. For higher weight fractions of TiO_2, the peaks were due to the π–π^* absorption of PPV and the band-gap onset of TiO_2, merge into a broad absorption band dominated by the TiO_2 absorption. The absorption spectra

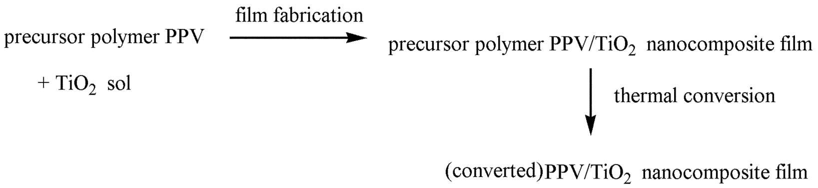

Fig. 2. Schematic diagram showing the steps involved in the formation of PPV/TiO_2 nanocomposite film from PPV precursor and TiO_2 sol.

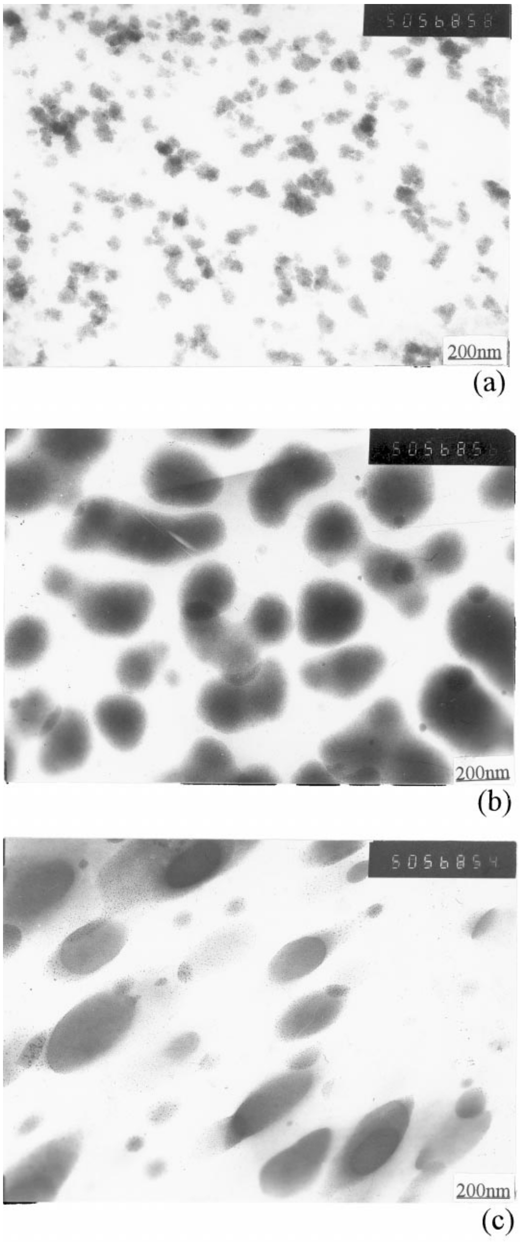

Fig. 3. TEM of PPV/TiO_2 nanocomposites: (a) PPV/TiO_2-A; (b) PPV/TiO_2-C; and (c) PPV/TiO_2-D.

were the sum of the absorption spectra of the two components individually, indicating that no ground-state charge-transfer or significant electronic interaction occurred between PPV and TiO_2 nanoparticles.

3.4. Photoluminescence spectra

The PL spectra have been normalized to the same maximum value for better comparison and both showed three discernible peaks. The thin dashed curve shows three Gaussians whose sum is fit to the PPV PL. The overall fit is indistinguishable from the data on the scale of the figure;

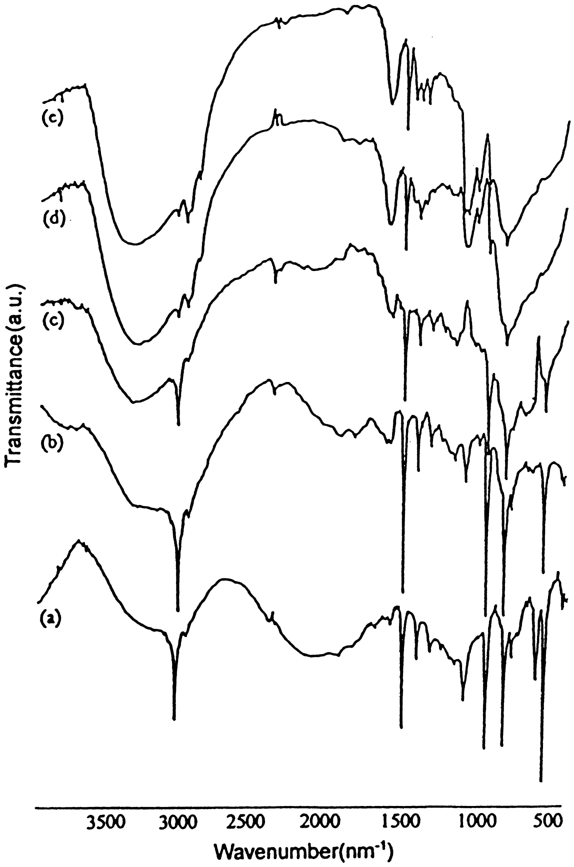

Fig. 4. FT-IR absorption spectra of PPV and PPV/TiO_2 nonocomposites: (a) PPV; (b) PPV/TiO_2-A; (c) PPV/TiO_2-B; (d) PPV/TiO_2-C; and (e) PPV/TiO_2-D.

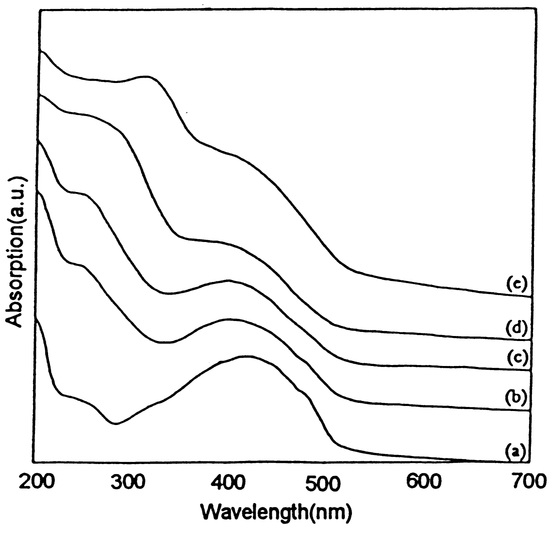

Fig. 5. UV–VIS absorption spectra of PPV and PPV/TiO_2 nanocomposites: (a) PPV; (b) PPV/TiO_2-A; (c) PPV/TiO_2-B; (d) PPV/TiO_2-C; and (e) PPV/TiO_2-D.

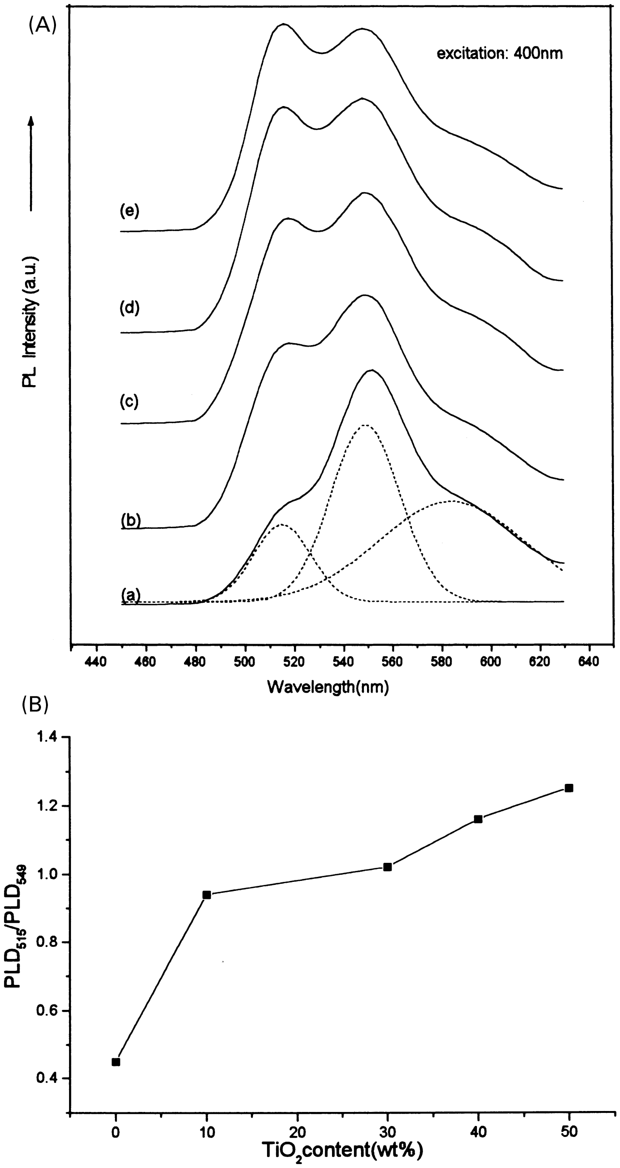

Fig. 6. (A) Photoluminescence spectra of PPV and PPV/TiO_2 nanocomposites: (a) PPV; (b) PPV/TiO_2-A; (c) PPV/TiO_2-B; (d) PPV/TiO_2-C; and (e) PPV/TiO_2-D. The small dashed curves show Gaussian fits to the three visible peaks of the PPV PL; fit parameters for the film PL are summarized in Table 2. (B) The effect of TiO_2 content on the PL intensity ratio of peak 1 (515 nm) to peak 2 (549 nm).

the Gaussian fit parameters for all of the PL spectra shown in Fig. 6A are summarized in Table 2.

For the PPV PL, it was known that PPV film emitted in yellow-green at 540 nm with vibrant side bands at 510 and 570 nm, which assigned to 0–1, 0–0, 0–2 transition, respectively [16]. The PPV/TiO_2 nanocomposites had same features as the pure PPV film, except the relative intensity of the vibrant components. As shown in Fig. 6B, the 0–0 (510 nm) peak enhanced and the 0–1 (540 nm) peak reduced with the increase of TiO_2 content. Because the TiO_2 nanoparticles had no PL in our experimental condition, the phenomenon suggested that the light emission of the PPV/TiO_2 nanocomposites was from PPV. The incorporation of TiO_2 nanoparticles to PPV could change the relative intensity of the vibrant components in the PL of PPV.

4. Discussion

It is well known that the titanium oxide nanoparticles are obtained by the TBT hydrolytic polycondensation reactions, which can be written as the following equations [15]:

$$nTi(OBu)_4 + (4n + x - y)H_2O \longrightarrow Ti_nO_{[2n-(x+y)/2]}(OH)_x \times (OBu)_y + (4n - y)Bu(OH) \quad (1)$$

Table 2
Fit parameters (each PL spectrum is fit to $\sum_{i=1}^{3} a_i \exp[-2((x-\lambda_i)/\sigma_i)^2]$) to normalized PL spectra of the PPV/TiO$_2$ nanocomposite films presented in Fig. 6A

TiO$_2$ content (wt%)	Peak 1	Peak 2	Peak 3
0	$\lambda_1 = 515$	$\lambda_2 = 548$	$\lambda_3 = 584$
	$\sigma_1 = 23.2$	$\sigma_2 = 28.3$	$\sigma_3 = 59.6$
	$a_1 = 0.35$	$a_2 = 0.70$	$a_3 = 0.40$
10	$\lambda_1 = 515$	$\lambda_2 = 548$	$\lambda_3 = 584$
	$\sigma_1 = 28.0$	$\sigma_2 = 28.0$	$\sigma_3 = 68.1$
	$a_1 = 0.65$	$a_2 = 0.66$	$a_3 = 0.42$
30	$\lambda_1 = 515$	$\lambda_2 = 548$	$\lambda_3 = 584$
	$\sigma_1 = 26.9$	$\sigma_2 = 28.9$	$\sigma_3 = 68.0$
	$a_1 = 0.70$	$a_2 = 0.63$	$a_3 = 0.44$
40	$\lambda_1 = 515$	$\lambda_2 = 548$	$\lambda_3 = 584$
	$\sigma_1 = 26.8$	$\sigma_2 = 28.1$	$\sigma_3 = 70.0$
	$a_1 = 0.80$	$a_2 = 0.64$	$a_3 = 0.43$
50	$\lambda_1 = 515$	$\lambda_2 = 548$	$\lambda_3 = 584$
	$\sigma_1 = 25.2$	$\sigma_2 = 28.3$	$\sigma_3 = 72.0$
	$a_1 = 0.86$	$a_2 = 0.67$	$a_3 = 0.42$

$$\mathrm{Ti}_n\mathrm{O}_{[2n-(x+y)/2]}(\mathrm{OH})_x(\mathrm{OBu})_y \rightarrow n\mathrm{TiO}_2 + x\mathrm{H}_2\mathrm{O} + y\mathrm{Bu(OH)} \tag{2}$$

where n was the number of titanium ions polymerized in a given condensation, and x and y were the numbers of OH and OBu groups in the molecule. The titanium oxide nanoparticles were coated with the Ti organic product $\mathrm{Ti}_n\mathrm{O}_{[2n-(x+y)/2]}(\mathrm{OH})_x(\mathrm{OBu})_y$ which consisted of groups, such as Ti–OH, Ti–O, Ti–O–C, as shown in the FT-IR spectra. In this case, the morphologies of titanium oxides were related with the conformation of the Ti organic product $\mathrm{Ti}_n\mathrm{O}_{[2n-(x+y)/2]}(\mathrm{OH})_x(\mathrm{OBu})_y$. As reported, the Ti organic product, $\mathrm{Ti}_n\mathrm{O}_{[2n-(x+y)/2]}(\mathrm{OH})_x(\mathrm{OBu})_y$ were more extended, less branched polymers under acid condition [15]. These inorganic polymers can result in the TiO$_2$ alignment structure. In sol–gel process, the TiO$_2$ matrix can act as confined environments to effect the aggregate states of PPV, since the TiO$_2$ matrix surface group, such as –OH, –OR, can interact with the tetrahydrothioohene group in PPV precursor polymer, the degree of dissociation between the chloride and the sulfonium ions will be greater in the TiO$_2$ matrix, which will lead to stronger coulombic repulsions along the polymer backbone and hence, an increase in the chain extension and reduction in the conformation defect. Therefore, thermal treatment of these films lead to the formation of a solid with a high degree of planariation [17].

The change in the PPV aggregate states can result in new spectroscopic features. In the PL spectra, the light emission of the PPV/TiO$_2$ nanocomposites was from PPV, and the incorporation of TiO$_2$ nanoparticles into PPV could change the relative intensity of the vibrant components. The phenomenon was different from that of Ref. [12], which considered that electron transfer happened at the interface between PPV and TiO$_2$ nanoparticles. In our work, the more reasonable possibility to account for the structural effects was that the excitons formed in the PPV of the composite had different configurational coordinate displacements and associated emission spectra with the increase of the TiO$_2$ content. It is known that the relative intensities of the vibronic components are determinated by the configurational coordinate displacement (ΔQ). As ΔQ decreases, the position of the peak in the vibronic spectrum will shift to lower vibrational state; when $\Delta Q \approx 0$, only the 0–0 transition will be dominated [18]. In our work, the TiO$_2$ nanoparticles aggregated in alignment configuration with the increase of the TiO$_2$ content. The confined environments of TiO$_2$ matrix generate a potential barrier against PPV molecular torsion and facilitate planarization. In this condition, the configurational coordinate displacement (ΔQ) reduced. Thus the 0–0 (510 nm) peak relative intensity of the composite film increased, while the 0–1 (540 nm) peak relative intensity reduced.

5. Conclusions

PPV has been incorporated into TiO$_2$ nanoparticles by employing a sol–gel process. The confined environment of TiO$_2$ matrix can influence the optical properties of PPV. When the TiO$_2$ content increases, the elliptical TiO$_2$ nanoparticles form alignment structure. The TiO$_2$ matrix can generate a potential barrier against PPV molecular torsion and facilitate planarization, which can reduce the configurational coordinate displacement (ΔQ) of PPV molecules, and lead to a change in the relative intensity of vibrant components in PPV PL spectra. The study also gives a new way to control the aggregate states of PPV and modulate the optical property of PPV by incorporating TiO$_2$ nanoparticles with different contents.

Acknowledgements

The research was supported by the 100-talent plan of Academia Sinica.

References

[1] Burroughes JH, Bradley DDC, Brown AR. Nature 1990;347:539–41.
[2] Benjamin I, Faraggi EZ, Avny Y. Chem Mater 1996;8:352–5.
[3] Faraggi EZ, Cohen G, Neumann R. Adv Mater 1996;8(3):234–6.
[4] Granstrom M, Inganas O. Appl Phys Lett 1996;68(2):147–9.
[5] Gurge RM, Sarker A, Lahti PM. Macromolecules 1996;29:4287–92.
[6] Maria A, Diaz G, Fumitomo H. Synth Met 1997;84:455–62.
[7] Lemmer O, Henning R, Guss W. Appl Phys Lett 1995;66(11):1301–3.
[8] Yessler N, Denton GJ, Friend RH. Nature 1996;382(22):695–7.
[9] Cao Y, Yu G, Heeger AJ. Adv Mater 1998;10:692–5.
[10] Gao MY, Richter B, Kirstein S. Adv Mater 1997;9:802–4.
[11] Colvin VL, Schlamp MC, Alivisatos AP. Nature 1994;370(4):354–6.
[12] Savenije TJ, Warman JM, Goossens A. Chem Phys Lett 1998;287:148–53.

[13] Salafsky JS. Phys Rev B 1999;59(16):10 885–90.

[14] Lenz RW, Han CC, Karasz FE. J Polym Sci A: Polym Chem 1988;26:3241.

[15] Brinker CJ, Scherer GW. Sol–gel science, the physics and chemistry of sol–gel processing. San Diego: Academic Press, 1990 (p. 42–9).

[16] Gagnon DR, Capistran JD, Karasz FE. Polymer 1987;28:567–73.

[17] Woodruff M. Synth Met 1996;80:257–61.

[18] Pope M, Swenberg CE, editors. Electronic process in organic crystals. New York: Oxford University Press, 1982. p. 143–53.